
Article:
Sun, R. and Burgess, I.W. orcid.org/0000-0001-9348-2915 (2016) An analytical and numerical prediction for ductility demand on steel beam-to-column connections in fire. Engineering Structures, 115. pp. 55-66. ISSN 0141-0296

https://doi.org/10.1016/j.engstruct.2016.02.036

AN ANALYTICAL AND NUMERICAL PREDICTION FOR DUCTILITY DEMAND ON STEEL BEAM-TO-COLUMN CONNECTIONS IN FIRE

Ruirui Sun[1] and Ian W Burgess[2]

ABSTRACT:

In this paper a simplified analytical method to assess the ductility demand on connections according to fire resistance requirements is developed on the basis of fundamental structural mechanics principles. An objective is to enable the development of a viable method to allow engineers to take the ductility of connections into account in design practice. Numerical finite element simulations of the single beam model were also performed to validate the simplified analytical model and reveal the important parameters that can influence the ductility demand within the connections. Using both analytical and numerical methods, the principal factors which influence the ductility demand of a connection, such as the span of the connected beam and the required connection strength, are also assessed. It is shown that:

1. The compressive ductility of connections is helpful in reducing the push-out of perimeter columns and the possibility of local buckling of beams;
2. Provision of high tensile deformation capacity allows large deflection in the beam, substantially reduces catenary forces on the connections, and consequently reduces the risk of structural collapse in fire;
3. The ductility demand of the connection is closely related to its stiffness and strength, as well as to the slenderness and load ratio of the connected beam.

KEYWORDS: Ductility demand, Connection, Structural Mechanics, Design Method, Fire.

[1] Structural Engineer, MMI Engineering Ltd, Aberdeen, AB12 3JG, Email: sr_1123@hotmail.com

[2] Professor, Department of Civil and Structural Engineering, the University of Sheffield, Sheffield, S1 3JD, UK, Email: ian.burgess@sheffield.ac.uk

Notation

A	area of the beam's cross-section
$D_{cu,T}$	Compressive deformation limit
$D_{tu,T}$	Normal tensile deformation capacity, or ductility
$f_{y,T}$	yield strength of steel at temperature T
$K_{B,T}$	axial stiffness of the beam at temperature T
$K_{c,20}$	axial compressive stiffness of the connection at ambient temperature
$K_{c,T}$	Initial stiffness in tension of a connection at temperature T
k_c	axial stiffness of each connection
$k_{E,T}$	degradation of elastic modulus due to temperature rise
$K_{JR,T}$	rotational stiffness of the connections
$K_{R,T}$	the rotational stiffness of the steel beam
$K_{t,T}$	Initial stiffness in tension of a connection at temperature T
$k_{y,T}$	reduction factor for the yield strength of steel at temperature T
E_T	Elastic modulus of steel at temperature T
I	Second moment of area of beam section
M_E	externally applied free bending moment at mid-span
M_I	bending moment at the mid-span of the beam
M_m	mid-span bending moment for a pin-ended beam of span l without restraint
$M_{P,T}$	moment capacity of the beam's cross-section at temperature T
$M_{Rd,20}$	moment capacity of beam section at ambient temperature
$M_{Rd,T}$	moment capacity of beam section at temperature T
M_R	moment at the left-hand connection
$M_{t,T}$	moment at the beam ends
$N_{C,T}$	Axial force in the connection at temperature T
$N_{Cmax,T}$	maximum axial compression force
$N_{CRd,T}$	axial compression capacity of the connection at temperature T
$N_{Rd,20}$	axial capacity of beam section at ambient temperature
$N_{Rd,T}$	axial capacity of beam section at temperature T
N_T	Axial force of a beam
$N_{TRd,T}$	Tensile capacity of a connection at temperature T
N_V	shear force at each beam-end connection
T	Temperature in fire
T_1	Temperature at which the connection contacts with the column flange
T_B	Temperature at point B in Figure 2
T_C	Temperature at point C in Figure 2

T_D	Temperature at point D in Figure 2
α	thermal expansion coefficient
θ	temperature change
δ_c	compressive deformation in the connection at temperature T
δ_S	accumulated mechanical strain of the beam
$\overline{\delta_{c,m}}$	normalized ductility of the connection up to its contact with the connected column
$\overline{\delta_{m,T}}$	normalized ductility of the connection at temperature T
ρ_T	the ductility factor at temperature T
δ_m	design ductility at ambient temperature
μ	load ratio of the beam, normalized with respect to its plastic moment capacity
ϕ	tensile capacity of the connection, normalized with respect to the plastic moment capacity of the beam
λ	slenderness ratio of the beam
r_s	radius of gyration
Δ	maximum (mid-span) deflection of the beam
β_c	axial restraint ratio of each connection
$\delta_{t,m}$	designed-in tensile ductility of the connection at ambient temperature
$\overline{\delta_{t,m}}$	normalized designed-in tensile ductility of the connection at ambient temperature
$\delta_{c,m}$	designed-in compressive ductility of the connection at ambient temperature
$\overline{\delta_{c,m}}$	normalized designed-in compressive ductility of the connection at ambient temperature

1 INTRODUCTION

After the events of 11 September 2001, the focus of research in structural fire engineering has gradually moved towards the robustness of structures in fire. The capacity of a structure to prevent fire-induced progressive collapse is now recognized as one of the more important criteria in performance-based structural fire engineering design. Structural integrity in fire is a rather complex issue, involving the strength and expansion performance of different materials under elevated temperatures, the behaviour of individual members and their interactions. Among the structural components that contribute to the robustness of a frame, beam-to-column connections have vital importance, since they bridge the horizontal and vertical members and provide the load paths from slabs and beams to columns. Restrained by surrounding structure, steel/composite beams can develop significant forces in the connections, which are not considered in the ambient-temperature design of the connections, when exposed to fire. In this sense, connections can be both the most vulnerable and the least adequately designed parts of a frame, having the potential to trigger progressive collapse in exceptional fire events. The failure of connections can also lead to loss of fire compartmentation, and consequently cause the spread of fire between compartments, which can trigger a catastrophic escalation of failures within the structure.

The current trend of fire engineering design has been to move away from prescriptive methods to performance-based methods, in which the behaviour of structural members and their interactions are embedded into the assessment of overall structural fire resistance. In advanced fire engineering design, large deformations are allowed, provided that structural integrity (robustness) is maintained [1]. Tests and numerical studies have revealed that catenary action in beams, which occurs at high deflection, can increase the structural resistance to avoid progressive collapse. Li *et al*. [2] conducted high-temperature experiments on axially restrained steel beams, in which significant axial forces were measured. Liu *et al*. [3] investigated the effect of restraint on steel beams, leading to the catenary action which might be able to prevent deflections from running away at very high temperatures, also

experimentally. Catenary action was observed in these tests, and it was clear that horizontal restraint and catenary action are both important to the behaviour of beams in fire conditions.

In order to utilize the catenary action in beams exposed to fire, one of the key issues is to retain the robustness of the connection under the complex set of internal forces caused by heating. Sufficient strength and ductility within the connections is clearly necessary to sustain these forces along with large deflections. Nevertheless, recent experimental studies [4, 5] have indicated that the conventional connections (endplates, fin plates and web cleats) exhibit relatively limited ductility under fire conditions. Thus, taking into account the ductility demand on connections at the design stage of a building is imperative in order to ensure their robustness when it is necessary to utilize beam catenary action in the event of a fire. Achieving sufficient ductility in connections to prevent the collapse of beams in fire will require: (1) a design method to quantify the ductility demand on the connection; (2) innovative design of the connection details such as bolts, endplates and their overall geometry.

Simplified methods to predict the behaviour of steel beams have been proposed by many researchers. Wang and Yin [6] used the finite element and simplified methods to predict the behaviour in fire of restrained steel beams. Their simplified method iteratively predicts the deflections and internal forces of beams on the basis of both equilibrium and a moment-axial force interaction. Tan and Huang [7] studied the fire-induced restraint forces in steel beams considering the effects of slenderness ratio, load utilization factor and thermal gradient across the steel section. Dwaikat and Kodur [8, 9] proposed a simplified approach to predict the fire-induced forces and deflections of restrained steel beams. This method applies equilibrium equations to obtain critical fire-induced forces, and then utilizes compatibility principles to obtain the temperature-deflection history of the beam. It is validated by comparing its predictions with results obtained from detailed finite element analysis. Although these proposed approaches might be applicable in practical design to assess a beam's behaviour in fire, none of them have taken the ductility within connections into account.

The intention of this study is to propose a simplified method to estimate approximately the ductility demand on a steel beam-to-column connection in fire. Such an estimate could potentially serve as a baseline for subsequent detailed connection design calculations for the fire limit state. Numerical finite element modelling of steel beams with connection at both

ends have been performed, firstly to validate the simplified analytical model and secondly to reveal the important factors which can influence the ductility demand within the connections. Using both analytical and numerical approaches, a series of parametric studies on the ductility demand on connections have been carried out. These have provided an initial view of how the designed-in ductility of connections, in both tension and compression, affects the robustness of structures in fire, and on how other parameters can affect the ductility demand on connections.

2. LIMITATIONS

In this study, a simplified estimation of the ductility demand on connections is derived from the behaviour of restrained beams in fire. An effective structural fire collapse analysis tool has been developed in the software *Vulcan* [10, 11, 12, 13], with which the sequence of progressive failure within connections can be tracked during the course of a fire. The software is here utilized, firstly to validate the approximation of ductility demand from the simplified method, and secondly to perform the parametric study on the factors that affect it in fire.

As discussed above, achieving the required ductility also relies heavily on the detailing of a connection. However, the simplified method proposed in this study is intended to estimate in a general manner the required plastic movement capacity (ductility) in tension and compression of a steel connection to achieve the desired fire resistance. It does not consider connection detailing directly, but can provide guidance on the ductility that the detailed design needs to achieve.

3. SIMPLIFIED CHARACTERISTICS OF A CONNECTION

In a simplified fashion, the essential characteristics of a beam-to-column connection in terms of its movements normal to the column flange can be illustrated as shown in Figure 1, in which ideal elastic-to-plastic characteristics in both compression and tension are assumed.

The terms defining its characteristics are:

- The initial stiffnesses $K_{t,T}$ and $K_{c,T}$ in tension and compression at temperature T;
- The tensile and compressive capacities $N_{TRd,T}$ and $N_{CRd,T}$;

- The tensile deformation at fracture $D_{tu,T}$, which is known the normal tensile deformation capacity, or ductility.
- The compressive deformation limit $D_{cu,T}$, at which it is assumed that the beam contacts the column flange directly, causing rapid increase of the compression force without fracture.

4 ANALYTICAL MODEL OF BEAM BEHAVIOUR IN FIRE

The typical response of a restrained beam in fire, illustrated in Figure 2, can be categorized into three main stages:

Stage 1 The axial compression force grows due to restrained thermal expansion, until it reaches an ultimate value at point B, due to a combination of material stiffness and strength degradation and thermal buckling;

Stage 2 The axial compression force gradually reduces to zero, because of further reduction of strength and plastic buckling;

Stage 3 Catenary tension develops in the beam.

The connection behaviour during each of these stages will be discussed in this section.

The connection behaviour during each of these stages will be discussed in this section. The most important assumptions made in the derivation of the analytical model are:

1. A beam supported at connections is subjected to uniformly distributed load;
2. There is no significant sagging deflection in the beam in Stage 1 (the thermal expansion stage);
3. The external axial restraint to the beam and its connections, provided by the surrounding structure, is infinite compared to the axial stiffness of the beam;
4. The moment capacities of the cross sections of the beam and its connections are assumed to follow the same reduction factor with temperature;
5. In the connection model, the locations of the tension and compression springs coincide, and therefore have the same lever-arm;

6. All beams are assumed to be straight and prismatic, and bending behaviour only occurs about the major axis. Neither local nor lateral-torsional buckling is considered.

For the sake of clarity, these assumptions will be reiterated in the text when they are applied in the derivation of the analytical model.

Figure 3 shows a steel beam with connections at its ends. Assuming that the beam is symmetrically loaded with a uniformly distributed load w, equilibrium of the left-hand part of the beam provides:

$$N_T\Delta - N_V l/2 + M_I + M_R + M_E = 0 \quad (1)$$

Where:

N_T is the axial force ($N_{C,T}$ in compression and $N_{T,T}$ in tension)

$N_V = \frac{wl}{2}$ is the shear force at each beam-end connection;

M_I is the bending moment at the mid-span of the beam;

M_R is the moment at the left-hand connection;

$M_E = \frac{wl^2}{8}$ is the externally applied free bending moment at mid-span;

l is the length of the beam;

Δ is the maximum (mid-span) deflection of the beam.

The beam's deformed shape can be considered as a symmetric parabola as the deflection develops. This can be defined as:

$$z(x) = 4\Delta\frac{x}{l}\left(1-\frac{x}{l}\right) \quad (2)$$

where, $z(x)$ is the vertical deflection at a distance x along the beam length. Then, the beam's elongation δ_E due to accommodating this deflected shape within its horizontal span is:

$$\delta_E = \int_0^l \left[1 + \left(\frac{dz}{dx} \right)^2 \right]^{1/2} dx - l = \frac{8\Delta^2}{3l} \tag{3}$$

Stage I

In this stage, the beam is assumed to expand as its temperature rises, without significant deflection. The connections at the beam ends are pushed towards the connected column flanges. The response of the beam is initially elastic, but properties degrade as its temperatures rises. The axial compression force $N_{C,T}$ in each connection is:

$$N_{C,T} = \alpha l \theta \frac{1}{\frac{2}{K_{c,T}} + \frac{1}{K_{B,T}}} = \frac{K_{c,T} K_{B,T}}{K_{c,T} + 2K_{B,T}} \alpha l \theta \tag{4}$$

where $K_{B,T} = \frac{E_T A}{l} = k_{E,T} E_{20} A / l$ is the axial stiffness of the beam at temperature T; $k_{E,T}$ is the degradation of elastic modulus due to temperature rise, $K_{c,T} = k_{E,T} K_{c,20}$ is the axial compressive stiffness of the connection at temperature T; α is the thermal expansion coefficient; l is the span of the beam; A is the area of the beam's cross-section; $\theta = T - 20$ is the temperature change. The compressive deformation in the connection δ_c is

$$\delta_c = \frac{K_{B,T}}{K_{c,T} + 2K_{B,T}} \alpha l \theta \tag{5}$$

If the compressive deformation of the connection is characterized in dimensionless terms as:

$$\overline{\delta_c} = \frac{\delta_c}{l} \tag{6}$$

Then

$$\overline{\delta_c} = \frac{K_{B,T}}{K_{c,T} + 2K_{B,T}} \alpha\theta \tag{7}$$

In the elastic stage, the moments at the mid-span and ends of the restrained beam, under uniformly distributed load w, are related to the restraints' rotational stiffness. The moments and deflections in the restrained beam can be predicted simply by interpolation between those of the same beam with pinned ends and those of the beam with fixed ends, in terms of the rotational stiffness of the beam's connections. The mid-span moment (M_m) and end moment (M_t) for beams with pinned or fixed ends can be given as follows:

$$M_m = \frac{wl^2}{8} \;;\; M_t = 0 \qquad \text{for beams with pinned ends;} \tag{8}$$

$$M_m = \frac{wl^2}{24} \;;\; M_t = \frac{wl^2}{12} \qquad \text{for beams with rigid ends;} \tag{9}$$

When the rotational stiffness of the connections is assumed to be $K_{JR,T}$, the mid-span moment and end moment of a restrained beam with connections can be approximately estimated as:

$$M_m = \left(1 - \frac{K_{JR,T}}{K_{R,T}}\right)\frac{wl^2}{8} + \frac{K_{JR,T}}{K_{R,T}}\frac{wl^2}{24} \tag{10}$$

$$M_t = \frac{K_{JR,T}}{K_{R,T}}\frac{wl^2}{12} \tag{11}$$

where $K_{R,T} = E_T I / l$ is the rotational stiffness of the steel beam.

If $\overline{k} = \dfrac{K_{JR,T}}{K_{R,T}}$ then

$$M_m = \left(1 - \overline{k}\right)\frac{wl^2}{8} + \overline{k}\,\frac{wl^2}{24} \tag{12}$$

$$M_t = \overline{k}\,\frac{wl^2}{12} \tag{13}$$

Assuming that the mid-span deflections of beams with pinned and fixed ends are $\Delta_1 = \frac{5wl^4}{384E_TI}$ and $\Delta_2 = \frac{wl^4}{384E_TI}$ respectively, the mid-span deflection Δ of a restrained beam with connections can be expressed as:

$$\Delta = (1-\bar{k})\Delta_1 + \bar{k}\Delta_2 = (1-\bar{k})\frac{wl^4}{76.8E_TI} + \bar{k}\frac{wl^4}{384E_TI} \tag{14}$$

The reduction of the compression force, indicating the end of the thermal expansion stage, can be induced by plasticity in the beam and its connections, or by buckling of the beam. If this is due to the spread of plasticity in the beam, the maximum axial compression force $N_{Cmax,T}$ in this stage can be conservatively determined as:

$$\frac{N_{Cmax,T}}{Af_{y,T}} + \frac{M_{m,T}}{M_{P,T}} = 1 \tag{15}$$

where $f_{y,T} = k_{y,T}f_y$ is the yield strength of steel at temperature T, $M_{P,T} = k_{y,T}M_P$ is the moment capacity of the beam's cross-section at temperature T, and $k_{y,T}$ is the reduction factor for the yield strength of steel at temperature T.

Then,

$$N_{Cmax,T} = \left(1 - \frac{M_{m,T}}{k_{y,T}M_P}\right)Ak_{y,T}f_y = \left(k_{y,T} - \frac{M_{m,T}}{M_P}\right)Af_y \tag{16}$$

If plasticity is allowed to develop in the connections, their stiffness is reduced, or may even vanish when the compressive force in the connections exceeds their compressive capacity $N_{CRd,T}$, shown in the characteristics in Figure 1. In such a case, the displacement of each connection is:

$$\delta_c = \left(\alpha l\theta - \delta_S\right)/2 \tag{17}$$

where $\delta_S = \frac{N_{CRd,T}}{K_{B,T}}$ is a conservative estimate of the mechanical shortening of the beam. Thus,

$$\overline{\delta_c} = \left(\alpha\theta - \frac{N_{CRd,T}}{k_{E,T} E_{20} A} \right) / 2 \tag{18}$$

$$N_{C,T} = N_{C,Rd,T} \tag{19}$$

If the compressive deformation of a connection reaches its deformation capacity $D_{cu,T}$, its compressive force increases rapidly, since the beam ends have come into contact with the connected column, at temperature T_1. If the stiffness of the axial restraint to the beam provided by the connected structure is assumed to be infinite, the deformation and compression force in the connection when it is in contact with the column are:

$$\overline{\delta_{c,m}} = \frac{D_{cu,T}}{l} \tag{20}$$

$$N_{C,T} = \alpha l \theta K_{B,T} \tag{21}$$

where $\theta = T - T_1$ and $\overline{\delta_{c,m}}$ is the normalized ductility of the connection up to its contact with the connected column, when the compressive force in the beam and its connections is reduced.

Stage II

The axial force in the connection gradually decreases as the beam's axialdeflection increases, and plasticity spreads within the beam during this stage. The end of this stage can be identified as the point at which the axial force in its connections becomes zero. The interaction between axial force and the moment in the connection may be simply represented (normally conservatively) as:

$$\frac{N_{C,T}}{N_{Rd,T}} + \frac{M_{R,T}}{M_{Rd,T}} = 1 \tag{22}$$

where $N_{Rd,T} = k_{y,T} N_{Rd,20}$ is the axial capacity and $M_{Rd,T} = k_{y,T} M_{Rd,20}$ is the moment capacity at temperature T. $N_{Rd,20}$ and $M_{Rd,20}$ are its axial capacity and moment capacity at ambient temperature. When $N_{C,T}$ reduces to zero, the moment in the connection reaches its full moment capacity at the temperature. Thus, the equilibrium of the beam can be represented by the following relationship:

$$-N_V l / 2 + M_{P,T} + M_{Rd,T} + M_E = 0 \tag{23}$$

If the moment capacity of a connection is assumed to follow the same reduction factor ($k_{y,T}$) with temperature as the moment capacity of the beam's cross-section, then Eqn. (23) gives,

$$k_{y,T} = \left(\frac{N_V l}{2} - M_E \right) / \left(M_{P,20} + M_{Rd,20} \right) \tag{24}$$

The temperature (T_C) at point C, shown in Figure 2, can be obtained from this reduction factor, from the temperature-strength reduction factor curve for structural steels, as given in Eurocode 3 Part 1.2 [14].

Stage III

During the catenary action stage, the normal forces carried by the connections become tensile. The tensile force on a connection increases until it reaches a maximum value, after which the connection is purely in tension with insignificant moment. With rising temperature, the load is then resisted by catenary action. This stage ends once the deformation of the connection exceeds its ductility, causing it to detach completely.

It can be seen from Figure 2 that, when the connection is purely in tension, its normal force (shown as Line 2) can be estimated as:

$$N_{TRd,T} = k_{y,T} N_{TRd,20} \tag{25}$$

A conservative approximation [9] of the maximum tensile force in the catenary stage is proposed by extending a straight line (Line 1 in Figure 2) between the point of maximum compressive force (B in Figure 2) and the point at which the catenary action starts (C in

Figure 2). The intersection point (D in Figure 2) of Line 1 and Line 2 is assumed to be the point at which the maximum tensile force occurs. The temperature T_D at which this maximum catenary force occurs in the beam is determined by:

$$\frac{T_D - T_C}{T_C - T_B} N_{Cmax,T} = k_{y,T_D} N_{Rd,20} \tag{26}$$

Then,

$$T_D = \frac{N_{Rd,20}}{N_{Cmax,T}} \frac{T_C - T_B}{k_{y,T_D}} + T_C \tag{27}$$

Before the temperature achieves the value T_D,

$$N_{t,T} = \frac{T - T_C}{T_C - T_B} N_{Cmax,T} \tag{28}$$

The interaction between axial force and moment in the connection gives:

$$M_{R,T} = \left(1 - \frac{N_{t,T}}{N_{Rd,T}}\right) M_{Rd,T} = k_{y,T} M_{Rd,20} - \frac{M_{Rd,20}}{N_{Rd,20}} N_{t,T} \tag{29}$$

As the temperature rises, the load-carrying mechanism gradually becomes that of a cable, in which the load on the beam is completely sustained by catenary tension. The equilibrium can be expressed as:

$$N_{TRd,T}\Delta + M_{P,T} - M_E = 0 \tag{30}$$

Then,

$$\Delta = \frac{M_E - M_{P,T}}{N_{TRd,T}} = \frac{M_E - k_{y,T} M_{P,20}}{k_{y,T} N_{TRd,20}} \tag{31}$$

The change of the beam's length is due to a combination of its thermal expansion, the ductilities of its connections and its mechanical strain. This can be expressed as:

$$\delta_E = \alpha\theta l + \delta_{m,T} + \delta_S \tag{32}$$

The mechanical deformations can conservatively be estimated as:

$$\delta_S = \frac{k_{y,T} N_{TRd,20} l}{k_{E,T} E_{20} A} \tag{33}$$

Substituting Eqns. (32) and (33) into Eqn. (3),

$$\Delta = \sqrt{\frac{3}{8} l \delta_E} = \sqrt{\frac{3}{8} l \left(\alpha\theta l + \delta_{m,T} + \frac{k_{y,T} N_{Rd,20} l}{k_{E,T} E_{20} A} \right)} \tag{34}$$

The displacement of the connections increases faster, because stiffness has been lost or reduced, at this stage. When the axial displacement in a connection exceeds its axial ductility the connection breaks and detaches from the connected column because of the fracture of its internal components.

The tensile ductility demand of the connection at elevated temperature can then be estimated as:

$$l\delta_{m,T} = \frac{8}{3} \left[\frac{M_E - M_{P,T}}{k_{y,T} N_{TRd,20}} \right]^2 - \alpha l^2 \theta - \frac{k_{y,T} N_{Rd,20} l^2}{k_{E,T} E_{20} A} \tag{35}$$

In dimensionless terms, this is equivalent to:

$$\overline{\delta_{m,T}} = \frac{8}{3} \left[\frac{\mu - k_{y,T}}{\phi l k_{y,T}} \right]^2 - \alpha\theta - \frac{k_{y,T} N_{TRd,20}}{k_{E,T} E_{20} A} = \frac{8}{3} \left[\frac{\mu - k_{y,T}}{\lambda \phi r_s k_{y,T}} \right]^2 - \alpha\theta - \frac{k_{y,T} N_{TRd,20}}{k_{E,T} E_{20} A} \tag{36}$$

where $\overline{\delta_{m,T}} = \frac{\delta_{m,T}}{l} = \rho_T \frac{\delta_m}{l}$ is the normalized ductility of the connection at temperature T; ρ_T is the ductility factor at temperature T; δ_m is the design ductility at ambient temperature; $\mu = \frac{M_E}{M_P}$ is the load ratio of the beam, normalized with respect to its plastic moment capacity,

$\phi = \frac{N_{TRd,20}}{M_P}$ is the tensile capacity of the connection, normalized with respect to the plastic moment capacity of the beam. Other terms are λ, the slenderness ratio of the beam and r_s, its radius of gyration, both about the beam's bending axis.

The ductilities of the connections play important roles in the thermal expansion stage (Stage I) and the catenary action stage (Stage III). In the thermal expansion stage, the compressive ductility determines the point at which the connection contacts the column flange, causing rapidly-increasing compression force in the beam. In the catenary action stage, the axial force in a connection, before its breakage, decreases as its tensile ductility increases. The demand for such ductility in connections is closely related to the beam's slenderness, the connection's capacity (strength), the cross-sectional properties of the beam and its loading.

5 Tensile and compressive ductility demands of the connections

In order to test the effects of these factors on the structural behaviour of steel beams, and the ductility demands which they place on their connections in fire, a study based on a simplified model is now carried out. It is difficult to evaluate the ductility of a complex connection in an accurate way, since it is determined and limited by so many different characteristics. A simplified connection model, shown in Figure 4(a), which consists of four rows of springs, is adopted to simulate a generic beam-to-column connection.

The model has upper and lower pairs of tension and compression springs separated by a lever-arm. The main aim is to understand in general terms the ways in which design of connections specifically to achieve a certain ductility could influence a structure's resistance to progressive collapse in fire. The generic model is relatively straightforward as a way of defining the ductility properties of a connection, and it is useful to reflect these ductilities in generic terms rather than by modelling a real connection in detail. The ductilities of each of the upper and lower bolt rows are defined in two parts; compressive and tensile. It is assumed that a bolt row fails when its tensile displacement exceeds the tensile ductility limit, but the stiffness of a bolt row becomes infinite when its compressive displacement reaches the compressive ductility limit. A beam with connections at both ends, as shown as Figure 4(b), heated by fire, is chosen as the basic model to investigate the effects of different factors

on the behaviour of the heated beam. As mentioned in Section 2.0, a finite element analysis has also been conducted using the computer program *Vulcan*. The beam is represented by 3-noded line elements with two Gaussian integration points along their length. The cross section of the beam is assumed to be UB *356×171×67*. It is assumed that the beam is uniformly heated following the standard fire curve. The temperature of the beam was obtained by a heat transfer calculation according to Eurocode 1 [15]. The temperature of the connection is the same as that of the beam. The yield strength of the steel is 275 MPa and the material degradation with temperature is defined following Eurocode 3 Part 1.2 [14] . The mesh size of the models involved in the following studies was set as 500 mm. Simplified (component-based) connection models are placed at the beam ends. The key properties of the components in the connection, as shown in Figure 1, are main parameters in this study and thus they are changed according to different study objectives as discussed in Section 5.1. Only ductile fracture of the connection components is considered in this study and these fractures are defined on the basis of the tensile deformation capability. Once the tensile deformation capability is exceeded, the connection component strength is reduced to zero to simulate the fracture.

To evaluate the degree of restraint given by the connection to the beam, it is convenient to define the axial restraint ratio as

$$\beta_c = \frac{k_c}{E_b A_b / l} \tag{37}$$

in which k_c is the axial stiffness of each connection, and $E_b A_b / l$ represents the beam's axial stiffness at ambient temperature. In this study, β_c ranges from 0.02 to 0.5. The slenderness ratios λ of beams are chosen as 20, 50, 75 to represent stocky to intermediate beams. Given that steel beams tend to be initially sized to a span:depth ratio of 20, and that the radius of gyration tends to be about 0.42-0.44 of the mean depth, the median slenderness ratio of 50 is in a fairly representative range. The designed-in moment capacity of the connection is represented by:

$$\mu_c = \frac{M_{Rd}}{M_P} \tag{38}$$

in which, M_{Rd} and M_P are respectively the plastic moment capacities of the connection and the beam at ambient temperature. Liu [3] studied the effect of the connection capacity on the limiting temperatures of unprotected beams, which is defined according to the criterion that the beam "fails" when its mid-span deflection exceeds $l/20$. It was concluded that moment-resisting connections can increase the limiting temperature of a beam compared with that of simply supported beams, but this benefit was limited by the capacity of the beam in the vicinity of the connection, where extensive tensile yielding near to the top of the web of the beam and local buckling of the bottom flange of the beam adjacent to the connection +were observed. The benefit diminishes when μ_c exceeds 0.667. In this study, μ_c ranges from 0.084 to 0.667.

In the generic connection model, only two bolt rows are considered, both of which can act in tension and compression. Under the assumption that both the tension and compression springs are in the same place, and therefore have the same lever-arm, the relationship between the axial capacity and the moment capacity can be simply evaluated as:

$$N_{Rd,20} = \frac{2M_{Rd,20}}{z} \tag{39}$$

where z is the lever arm. Thus, the designed-in axial capacity of the connection can be characterized as:

$$\phi = \frac{N_{Rd,20}}{M_P} = \frac{2\mu_c}{z} \tag{40}$$

All beams are assumed to be straight and prismatic, and bending behaviour only occurs about the major axis. Neither local nor lateral-torsional buckling is considered. The load ratio for a Class 1 cross-section of a pin-ended beam sustaining a uniformly distributed load w is defined at ambient temperature as

$$\mu = \frac{M_m}{M_P} \tag{41}$$

where $M_m = wl^2/8$ is the mid-span bending moment for a pin-ended beam of span l without restraint. The mid-span moment is normally less than $wl^2/8$ for a beam with semi-rigid

connections. In this study the load ratio for a restrained beam is kept the same as that for a pin-ended beam, to provide a basis for comparison. The load ratio μ takes the values 0.30, 0.50 and 0.70 in this study. The designed-in tensile or compressive ductility in each connection is characterized as

$$\overline{\delta_{t,m}} = \frac{\delta_{t,m}}{l} \quad \text{or} \quad \overline{\delta_{c,m}} = \frac{\delta_{c,m}}{l} \tag{42}$$

where $\delta_{t,m}$ and $\delta_{c,m}$ are the designed-in tensile and compressive ductilities of the connection at ambient temperature.

In this context an idealized predefined temperature field, which avoids heat transfer analysis, was directly applied to the structure. Thus, instead of a nonlinear analysis in the time domain, the analysis can more easily be conducted within the temperature domain.

5.1 Ductility demand in catenary action

From Eqn. (36), the properties affecting the tensile ductility demand of a beam connection include: the beam's load ratio, the beam's slenderness ratio and a connection's tensile strength. In this section the influences of different parameters are evaluated. Firstly, the effects of the stiffnesses, strengths and ductilities of the connections are discussed. Then, the influences of the slenderness ratio and load ratio of the beam on the connections' ductility demand are studied.

Stiffness, Strength and Ductility

Three key properties (initial stiffness, strength and ductility) are generally considered in the design of connections at ambient temperature. In order to test which are the key parameters with respect to the robustness of connections in fire, several analyses are carried out based on a uniformly heated beam with slenderness ratio of 50 and load ratio of 0.5, but with connections of different stiffness, strength and ductility.

Table 1 shows the values of the key parameters defined for the different connections, and the failure temperatures at which complete detachment of any connection occurs. It indicates that connections with different stiffnesses, but the same strengths and ductilities, generate very similar failure temperatures. The initial stiffness of a connection does not play an important

role in enhancing its robustness, which is mostly related to the fracture of its components and fracture of the connection. The strength and ductility of a connection have much greater influence than stiffness on its failure temperature. Higher strength and higher ductility can each retain the integrity of a connection to higher temperatures in fire. This demonstrates that, for a connection with a given strength, a higher ductility is required to achieve a higher failure temperature. Alternatively, for a connection with a given ductility, a higher failure temperature requires higher connection strength.

Figure 5 shows the beam deflection at mid-span and the axial force in the connection against temperature for an analyzed beam of slenderness ratio 50, derived from the finite element analysis. The abrupt increase of mid-span deflection and the decrease of the connection axial force are due to fracture of the connection. The plastic axial capacity of the connection, $N_{TRd,T} = k_{y,T} N_{Rd,20}$, which represents the maximum plastic axial capacity that can be attained by the connection in catenary action, is also plotted. It can be seen that the catenary force decreases as the deflection and temperature increase. If the tensile ductility of the connections is sufficient, then collapse of beams can be avoided within a specified temperature range.

Strengths and ductilities are the key factors which enable connections to retain their integrity in fire. Since this study is concerned with the influence of ductility on resistance to progressive collapse in fire, all of the following case studies in this section focus solely on how the change of tensile ductility (rather than strength) of connections, affects the behaviour of the supported beams.

Slenderness Ratio

Beams of different slenderness ratios are tested. Since all the beams in this study have the same cross-section, different slenderness ratios represent different beam spans. The same load ratios are adopted for these beams. Figure 6 shows the change of ductility demand of connections of strength ratio μ_c=0.334 to beams with different slenderness ratios, for different required failure temperatures. The solid line in each case represents the results from finite element analysis, and the dashed line shows the results from Eqn. (36). It can be seen that Eqn. (36) generally gives a conservative estimate of the ductility demand of connections over

most of the range of failure temperatures. The differences between these results become larger as the ductility increases. This is because, in Eqn. (36) the term $\frac{k_{y,T}N_{TRd,20}}{k_{E,T}E_{20}A}$, which represents the mechanical strain in the beam, is calculated using the reduced initial modulus $k_{E,T}E_{20}$, although the stress-strain curve is highly curvilinear at high temperatures. A more realistic estimate of the mechanical strain would give a much higher value, which would reduce the ductility demand more, and the simplified method curves in Figure 6 would close in towards the FE curves.

With a given normalized ductility provided by the connections, longer beams can survive for longer periods in fire, which equates to higher failure temperatures. It should be noted that, because the definition of normalized ductility is that given in Eqn. (42), a certain value of normalized ductility implies higher deformation capacity for connections to longer beams than to shorter beams. In the catenary action stage, the tensile force is dependent on the transverse load carried by the beam, and its deflection magnitude. The cases shown in Figure 6 all have the same load ratio, but with connections of the same ductility, larger spans can obviously generate larger mid-span deflections, which means that lower catenary tensions may be needed to keep the connections robust at any given temperature. Thus, with the same cross-section and the same load ratio, beams with longer spans require less normalized ductility, as defined in Eqn. (36), to achieve the same failure temperature.

Load Ratio

Figure 7 shows the ductility demands of connections to beams of various load ratios and different slenderness ratios. Obviously, the ductility demand increases with load ratio. The heavier load on the beams requires a higher tension in the catenary action stage to maintain robustness. Therefore, beams of higher load ratio require more tensile ductility in connections for any given strength before fracture occurs.

Figure 8 shows the development of the normal forces in connections as temperatures increase for different cases of load ratio. It indicates that increased load ratios reduce the magnitude of normal force in the connection in the two initial stages, but increase the normal force in the catenary action stage. The bending moments at mid-span of the beams with higher load ratios

are higher than those of the beams with lower load ratios. From Eqn. (16), the maximum compressive forces in the beams, before plastic bending develops, are lower with higher mid-span bending moments. The temperature at which the beams step into catenary action is lower for higher loads.

5.2 Ductility demand in thermal expansion stage

According to the discussion in Section 2.2, the compressive ductility of a connection, which represents its deformation capacity in compression, defines the point at which the connection contacts the connected column. This contact induces stiffer restraint to the beam's thermal expansion. This may cause two negative effects: firstly, the large compression force generated by this restraint can push columns, especially those at the edge of the building, outwards and therefore reduce their buckling capacities somewhat; secondly, this compression force can induce buckling or plasticity to develop within the beam.

The end of the thermal expansion stage can occur due to plasticity being developed in the beams (in line with the discussion in Section 2.2) which reduces their net compression forces. If plasticity is allowed to develop first in the connections, the maximum compression in the beam (at Point B in Figure 2) can be estimated as:

$$N_{Cmax,T} = \left(1 - \frac{M_{t,T}}{M_{Rd,T}}\right) N_{CRd,T} \tag{43}$$

where, $M_{t,T}$ is the moment at the beam ends, $M_{Rd,T}$ and $N_{CRd,T}$ are respectively the moment capacity and the axial compression capacity of its connections. This indicates that introducing plasticity and ductility into the connection characteristics can effectively reduce the axial compression in beams under fire conditions. The effects of the compressive ductility are studied here on the basis of beams with cross-sections of UB 356×171×67, slenderness ratio 50 and load ratio 0.5. The connections at the ends of these beams have the same initial compressive axial stiffness. The connections in Case 1 are assumed to be elastic in compression, with constant compressive axial stiffness. In Cases 2 and 3, both plasticity and deformation are allowed to develop in the connections. The properties of these connections are listed in Table 2.

Figure 9 shows the axial forces in the beam for the three different cases. The maximum compression appears in Case 2, because of the increase in restraint stiffness after the beam has contacted the connected column. The connections in Case 3 are designed with sufficient deformation capacity for the axial compression in the beam to be less than that in the other cases. The significant reduction in the axial force in the beam in Case 3, compared to that in Cases 2 and 1, is attributed to the allowable deformation capacity (the ductility in the connections). The connections move towards the column flange due to the thermal expansion of the beam. The connections in Case 3 possess sufficient compressive ductility to allow the movement, and so the expansion of the beam due to the temperature rise is not restrained. However, lower compressive ductility in the connections of Case 2 limit the movements of the connections due to thermal expansion, and induce contact between the connection and the column flange. The restrained thermal expansion leads to a significant increase in the axial force in the beam. It is evident that this axial compression in the beam due to restrained thermal expansion can be effectively reduced by introducing plasticity and sufficient ductility into the connections..

If the beam is elastically restrained, the key factors which affect its behaviour in fire include the compressive restraint stiffness, the beam's axial stiffness and its slenderness ratio. The effects of these factors have been studied by several researchers [2, 3, 7, 8, 9] , and it can be concluded that, in general, higher axial restraint stiffness induces higher compressive forces in the heated beams during their thermal expansion stage. Restrained beams with connections of different compressive stiffness are now tested, and the compressive deformations in the connections are investigated. Again, the beams are assumed to have the same cross-section (UB 356×171×67) and load ratio (0.5). The tensile properties of the connections are assumed to be the same. Beams with three different slenderness ratios are studied. All the connections are assumed to be elastic in compression. Table 3 lists the compressive stiffnesses of the connections for different cases. The compressive deformations in the connections for these different cases are shown in Figure 10. The compressive deformations in the connections are normalized with respect to the length of the beam, so that:

Normalized compressive deformation = (Compressive connection deformation / Beam Length)

It can be seen that, for beams with connections which are elastic in compression, higher stiffness ratios β_c generate smaller compressive deformations in the connections in their thermal expansion stages; this is also indicated by Eqn. (7). This is to say; if a connection is elastic in compression, its compressive ductility demand reduces as its stiffness increases.

Figure 11(a) shows the development of compressive deformation in the connection during the thermal expansion stage of Cases: 20-2, 50-2 and 75-2, which have beam slenderness ratios of 20, 50, and 75 respectively. This comparison illustrates the effect of the length of the beam on the development of compressive deformation within the connections. The axial compressive forces in the connection in these cases are also plotted against temperature in Figure 11. It can be seen that, in the thermal expansion stage, the longer beams generate larger compressive deformations in the connections, and so require more compressive ductility in order to avoid the connections contacting the connected column. Figure 11 (b) shows the compressive deformation of the connections, normalized with respect to the length of the beam, against temperature. It can be seen from Figure 11 that the normalized compressive deformations are almost identical for these cases, and are independent of the beam span in their thermal expansion stages, which is explained by Eqn. (18).

According to Eqn. (18), if plasticity is allowed to develop in the connections, their ductility demand, in order to reduce the axial force in the connected beam, is also related to their axial compressive capacities. The effect of the compressive axial strength of the connections on their compressive ductility demand is now studied. Table 4 lists the properties of the connections in different cases. In these cases, in order to study the development of the compressive deformation in the connections, it is assumed that the beam does not come into contact with the column flange.

Figure 12 shows the normalized compressive axial deformations of the connections in each case as temperature increases. This indicates that, if the connection is designed with less strength, it develops more compressive deformation with temperature rise in the thermal expansion stage, and therefore it needs higher compressive ductility to avoid contacting the connected column.

6 Discussion

When exposed to fire, restrained steel beams develop significant compressive internal force because of their thermal expansion, and the restraint maintains the robustness of the beam by resisting tension in the later catenary stage. Currently, restrained beams are typically designed as simple beams at ambient temperature, and the design approaches do not account for the factors that influence the behaviour of beams in fire. The numerical studies presented above illustrate that the ductility and strength of connections have a significant influence on the response of restrained beams under fire conditions. These factors should be taken into consideration in evaluating the robustness of restrained beams.

The current study shows that a proper design approach, which considers carefully the ductility and strength of connections, can help restrained beams to achieve better fire resistance. The designed-in tensile ductility of connections can reduce the catenary forces in beams and thus improve their fire resistance. Equally, designed-in compressive ductility can reduce the compressive forces in the heated beams due to their thermal expansion, and therefore local buckling of the heated beams and the push-out effect on their connected columns are less likely, or at least less severe. This indicates that connections with designed-in ductility, both in tension and compression, can enhance the robustness of steel beams and the integrity of the whole frame in fire. Simplified methods can also adequately predict the ductility demand of connections, for predicted temperature regimes. However, more detailed analysis and experimental studies are needed to quantify the effects of these ductilities, and how to change the ductility of any particular connection.

7 Conclusion

Ductility within a connection denotes its deformation capacity. The ductile design of connections is important for enhancement of structural robustness, since it relates to their deformation capacity. A simplified model to predict the ductility demand of connections in fire has been proposed. In order to test the influence of the ductility of connections on the structural behaviour of beams under fire conditions, parametric studies using a simplified connection model have been performed. The results of both the parametric studies and the simplified method predictions indicate that the compressive ductility of connections is helpful

in reducing the push-out of perimeter columns and the possibility of local buckling of beams. Tensile ductility contributes more to avoiding total connection failure and enhancing a structure's robustness, by reducing the catenary forces necessary for beams to carry their loads at high temperatures. Provision of higher deformation capacity in the connections allows larger deflection in the supported beams, substantially reducing the catenary forces in the connections and consequently reducing the risk of structural collapse in fire.

References

1. Sun, R.R., Burgess, IW. , Huang, Z.H. and Dong, G., "Progressive Failure Modelling and Ductility Demand of Steel Beam-to-Column Connection in Fire", *Engineering Structures*, 2015; 89:66-78.
2. Li, G.Q., He, J.L., and Jiang, S.C. (2000), "Fire-resistant experiment and theoretical calculation of a steel beam", *China Civil Engineering Journal* 32(4): 23-26.
3. Liu, T.C.H., Fahad, M.K. and Davies, J.M. (2002), "Experimental investigation of behaviour of axially restrained steel beams in fire", *Journal of Constructional Steel Research* 58(9): 1211–1230.
4. Burgess, I.W., Davison, J.B., Huang, S.S. and Dong, G., 'The Role of Connections in the Response of Steel Frames to Fire', *Structural Engineering International,* **22** (4)*,* (2012) pp449-461.
5. Yu, H.X., Burgess, I.W., Davison, J.B. and Plank, R.J., 'Experimental and Numerical Investigations of the Behaviour of Flush Endplate Connections at Elevated Temperatures',*Journal of Structural Engineering,* A*SCE,* **137** (1), (2011) pp 80-87.
6. Wang, Y.C. and Yin, Y. Z. (2006), "A simplified analysis of catenary action in steel beams in fire and implications on fire resistant design", *Steel and Composite Structures* 5(6): 367-386.
7. Tan, K.H. and Huang, Z.F. (2005), "Structural responses of axially restrained steel beams with semirigid moment connection in fire", *Journal of Structural Engineering* 131(4): 541-551.
8. Dwaikat, M. and Kodur, V. (2011), "Engineering Approach for Predicting Fire Response of Restrained Steel Beams", *Journal of Engineering Mechanics* 137(7): 447-461.
9. Dwaikat, M. and Kodur, V. (2011), "A performance based methodology for fire design of restrained steel beams", *Journal of Constructional Steel Research* 67(3): 510–524.
10. Sun RR, Huang ZH, Burgess IW., "Progressive collapse analysis of steel structures under fire conditions", *Engineering Structures*, 2012; 34:400–13.
11. Sun, R.R., Huang, Z.H. and Burgess, I.W., "The collapse behaviour of braced steel frames exposed to fire", *Journal of Constructional Steel Research*, 2012; 72:130–42.
12. Sun, R.R., Huang, Z.H. and Burgess, I.W., "A static/dynamic procedure for collapse analysis of structure in fire", *Proc. Fire Safety Engineering in the UK: The State of the Art,*2010; 37-42.

13. Sun, R.R., 'Numerical Modelling for Progressive Collapse of Steel Framed Structures in Fire', PhD thesis, University of Sheffield, November 2012.
14. European Committee for Standardization (CEN), *BS EN 1993-1-2, Eurocode 3: design of steel structures, Part 1.2: General rules- structural fire design*, British Standards Institution, UK, 2005.
15. European Committee for Standardization (CEN), *BS EN 1991-1-2, Eurocode 1:Actions on structures-Part 1-2: General actions – Actions on structures exposed to fire*, British Standards Institution, UK, 2002.

Table List:

Table 1 Failure temperatures (°C) of cases with different stiffness, strength and ductility

λ	β_c	μ_c	$\overline{\delta_{t,m}}$				
			0.005	0.01	0.03	0.05	0.07
50	0.02	0.084	619	639	677	703	749
		0.167	637	671	719	763	799
		0.334	665	705	779	835	893
		0.667	699	783	857	937	No failure
	0.1	0.084	625	639	675	701	747
		0.167	649	671	719	763	799
		0.334	673	711	781	835	893
		0.667	701	771	861	941	No failure
	0.5	0.084	626	640	677	705	745
		0.167	651	671	719	763	800
		0.334	674	712	783	837	892
		0.667	705	772	860	943	No failure

Table 2 Properties of connections in compression in different cases

Cases	Initial Axial Stiffness (β_c)	Axial Compressive Strength(ϕ)	Compresive Ductility($\overline{\delta_{t,m}}$)
Case 1	0.42	------	------
Case 2	0.42	0.002	0.0015
Case 3	0.42	0.002	0.0030

Table 3 Properties of connections in compression and slenderness ratio for different cases

Slenderness ratio(λ)	Compressive Axial Stiffness (β_c)	Cases
20	0.21	20-1
	0.42	20-2
	0.84	20-3
50	0.21	50-1
	0.42	50-2
	0.84	50-3
75	0.21	75-1
	0.42	75-2
	0.84	75-3

Table 4 Properties of connections in compression in Case A, B and C

(*z=350mm* is the lever-arm of the connections)

Slenderness ratio(λ)	Compressive Axial Strength (ϕ)	Compressive Axial Strength (β_c)	Cases
50	0.3/*z*	0.42	A
	0.5/*z*	0.42	B
	0.7/*z*	0.42	C

Figure Captions

Figure 1 Simplified characteristics of a connections

Figure 2 Typical curve of normal force (N) in an axially restrained beam against temperature.

Figure 3 Equilibrium in a heated connected beam

Figure 4 (a) Generic connection model (T: tensile springs; C: compression springs); (b) The beam with these connections at each end.

Figure 5 Mid-span beam displacement and axial force in connection against temperature: (a) Mid-span displacement of beam; (b) Normal force in connection

Figure 6 Ductility demand of the connections of strength ratio □c=0.334 on beams with different slenderness.

Figure 7 Ductility demand ($\overline{\delta_m}$) for connections to beams of various load ratios with different slenderness.

Figure 8 Normal forces in connections to beams with different load ratios.

Figure 9 Axial forces at mid-span of the beam for different cases

Figure 10 Normalized compressive deformation in the connections for different cases.

Figure 11 Compressive deformation (a) and normalized compressive deformation (b) in the connections for different cases

Figure 12 Compressive deformation in the connections for different cases

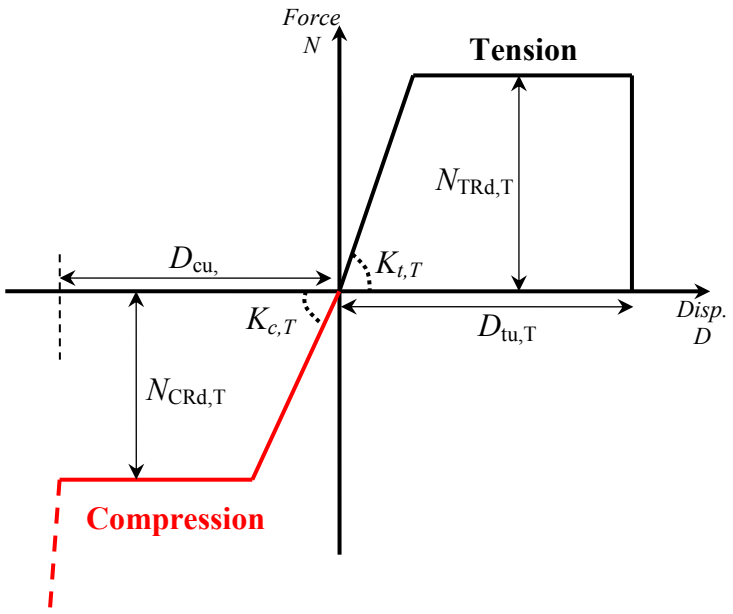

Figure 1 Simplified characteristics of a connections

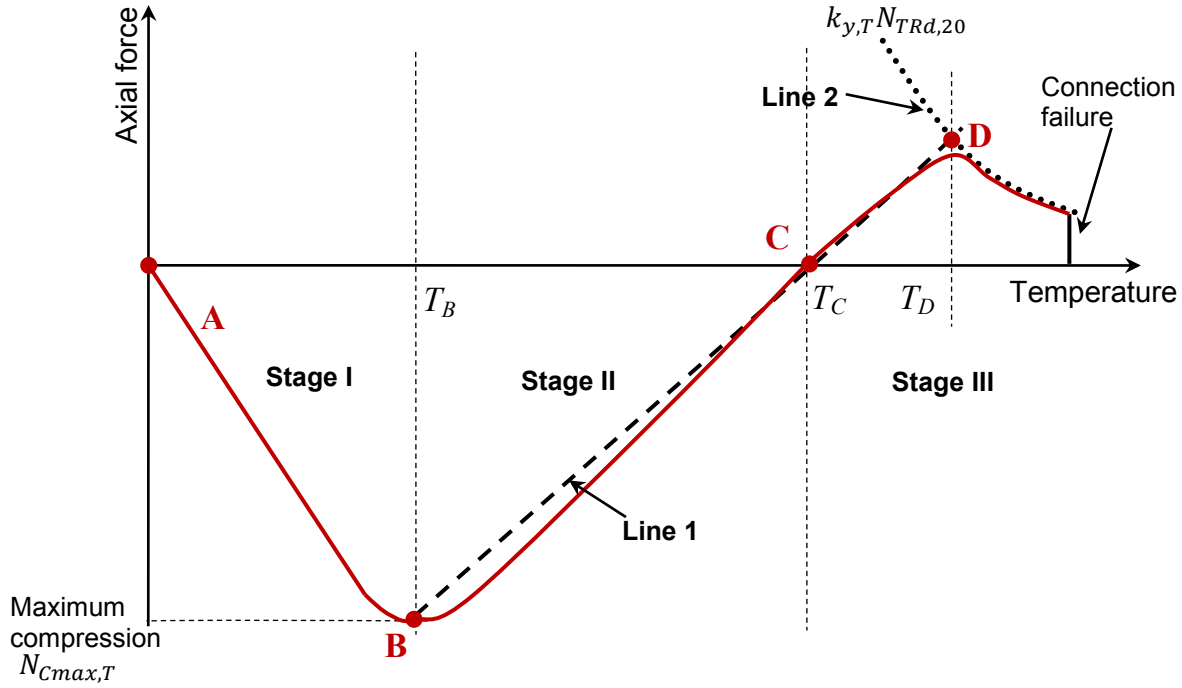

Figure 2 Typical curve of normal force (N) in an axially restrained beam against temperature.

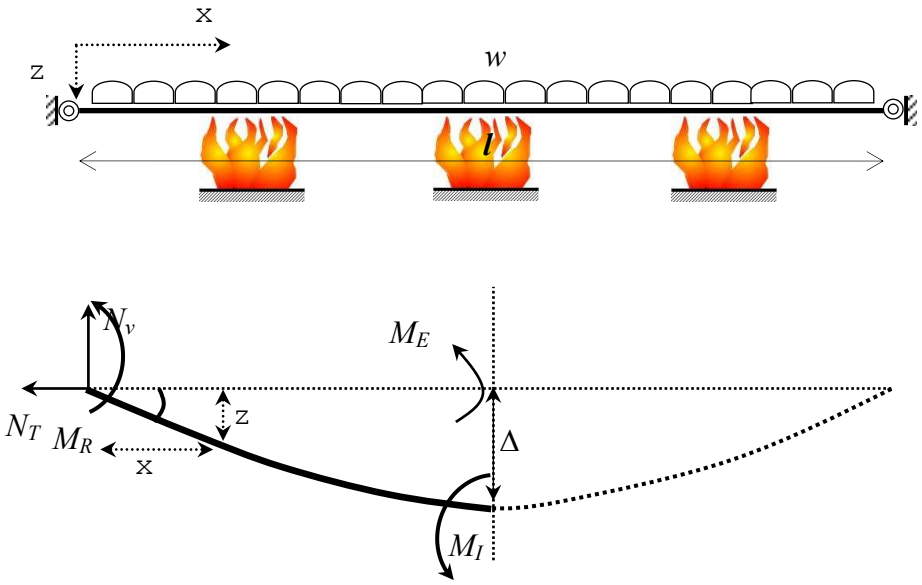

Figure 3 Equilibrium in a heated connected beam

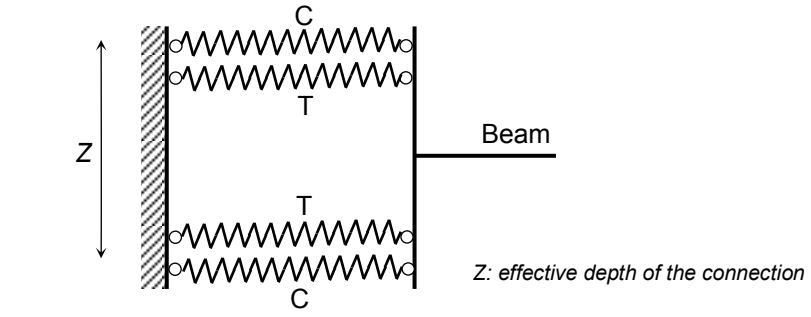

(a)

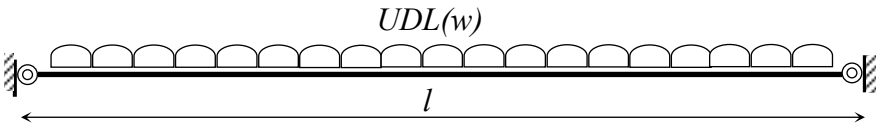

(b)

Figure 4 (a) Generic connection model (T: tensile springs; C: compression springs); (b) The beam with these connections at each end.

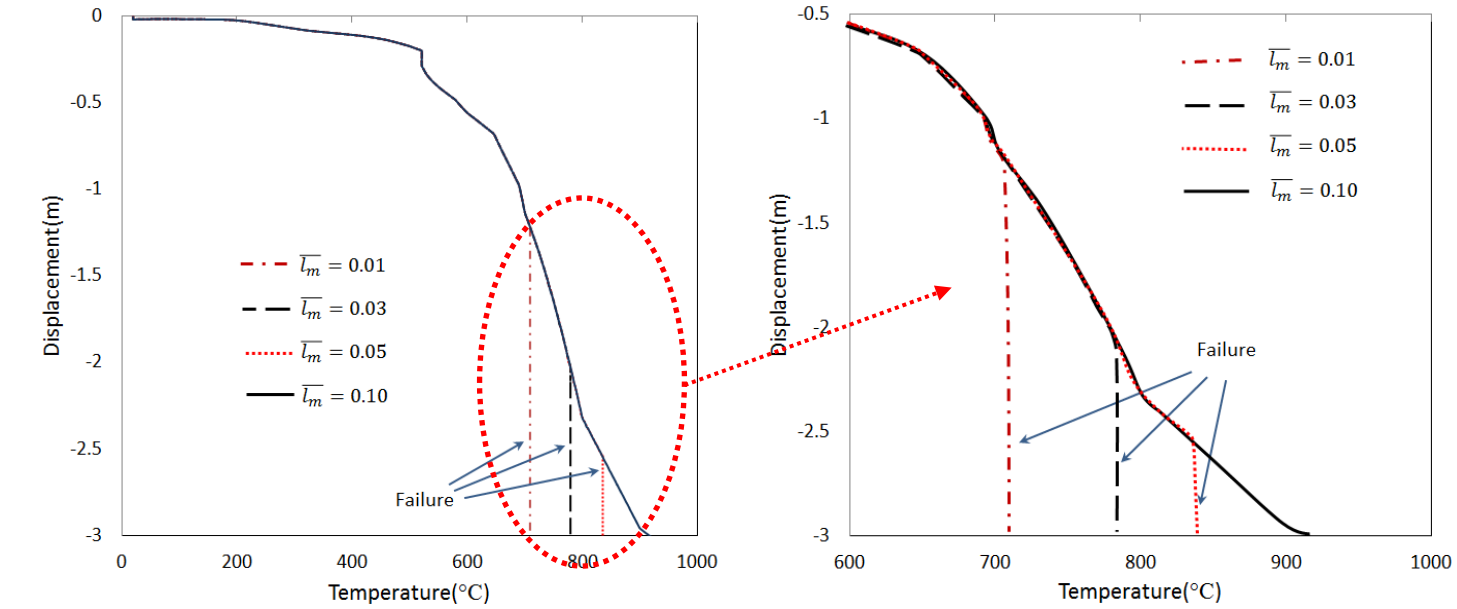

(a)

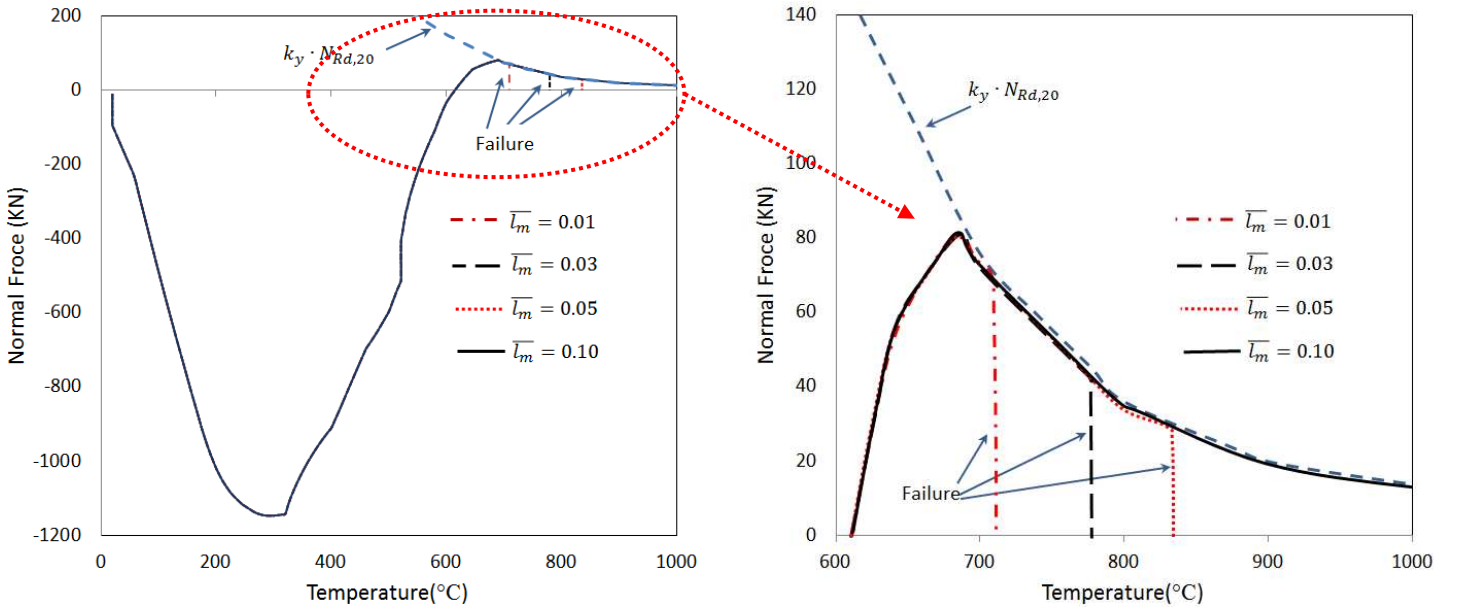

(b)

Figure 5 Mid-span beam displacement and axial force in connection against temperature: (a) Mid-span displacement of beam; (b) Normal force in connection

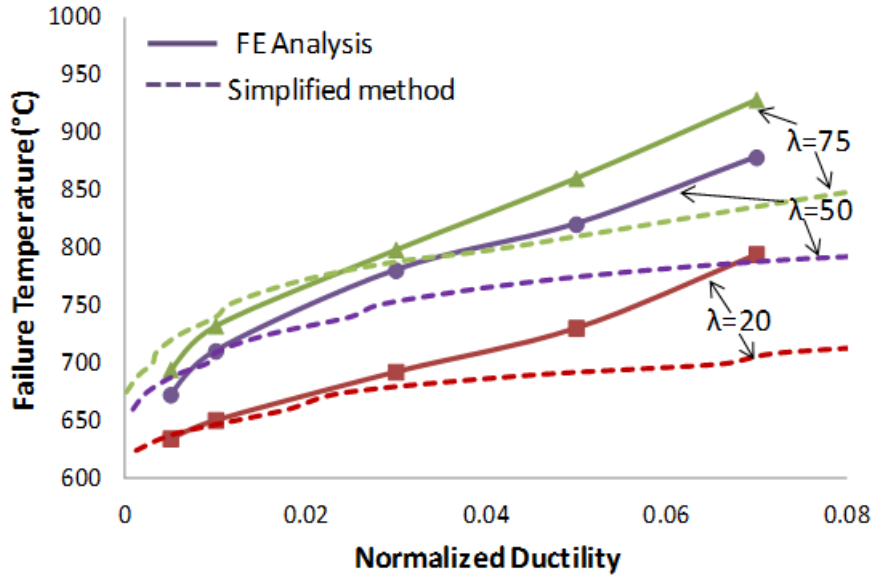

Figure 6 Ductility demand of the connections of strength ratio μ_c=0.334 on beams with different slenderness.

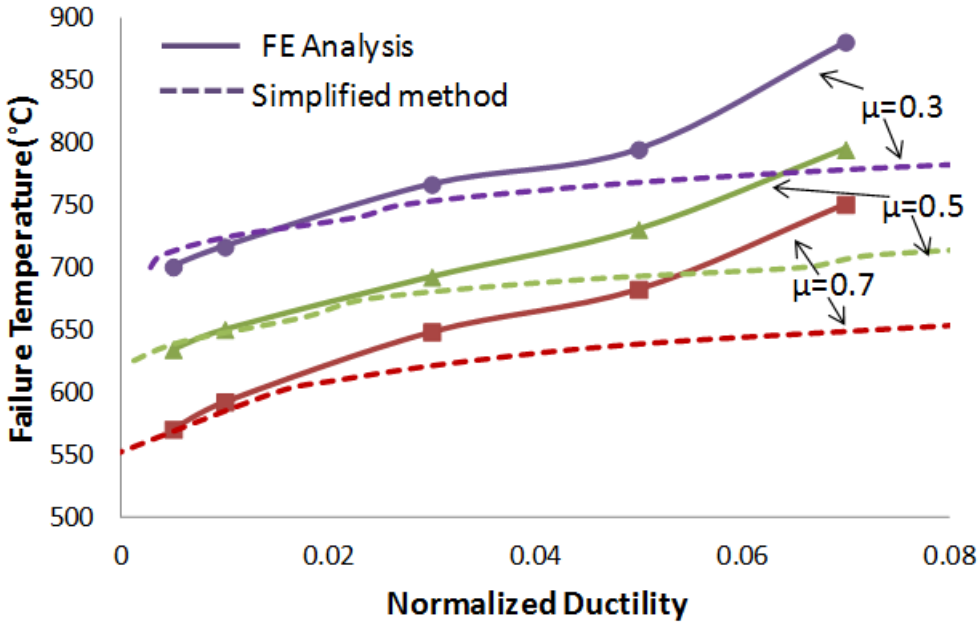

(a) $\lambda = 20$

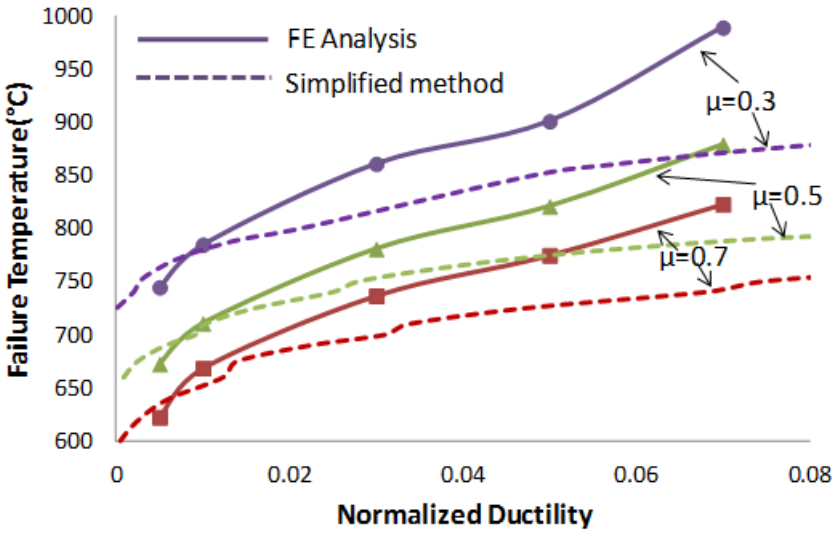

(b) $\lambda = 50$

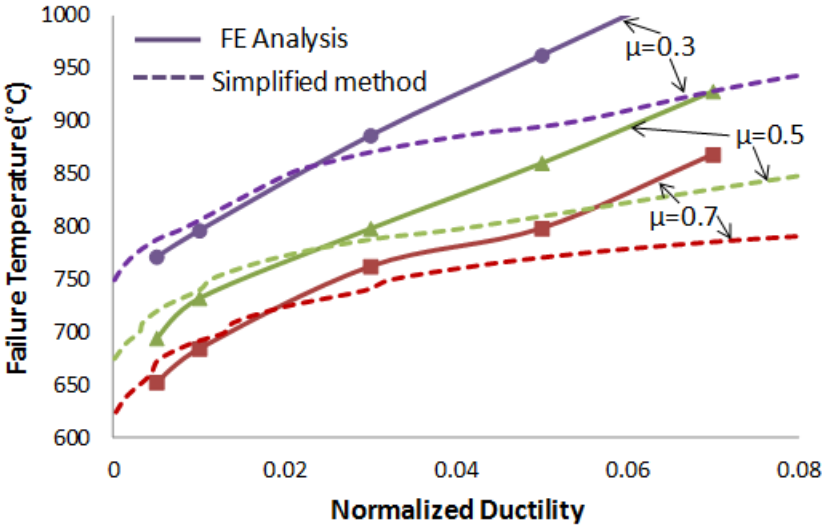

(c) $\lambda = 75$

Figure 7 Ductility demand ($\overline{\delta_m}$) for connections to beams of various load ratios with different slenderness.

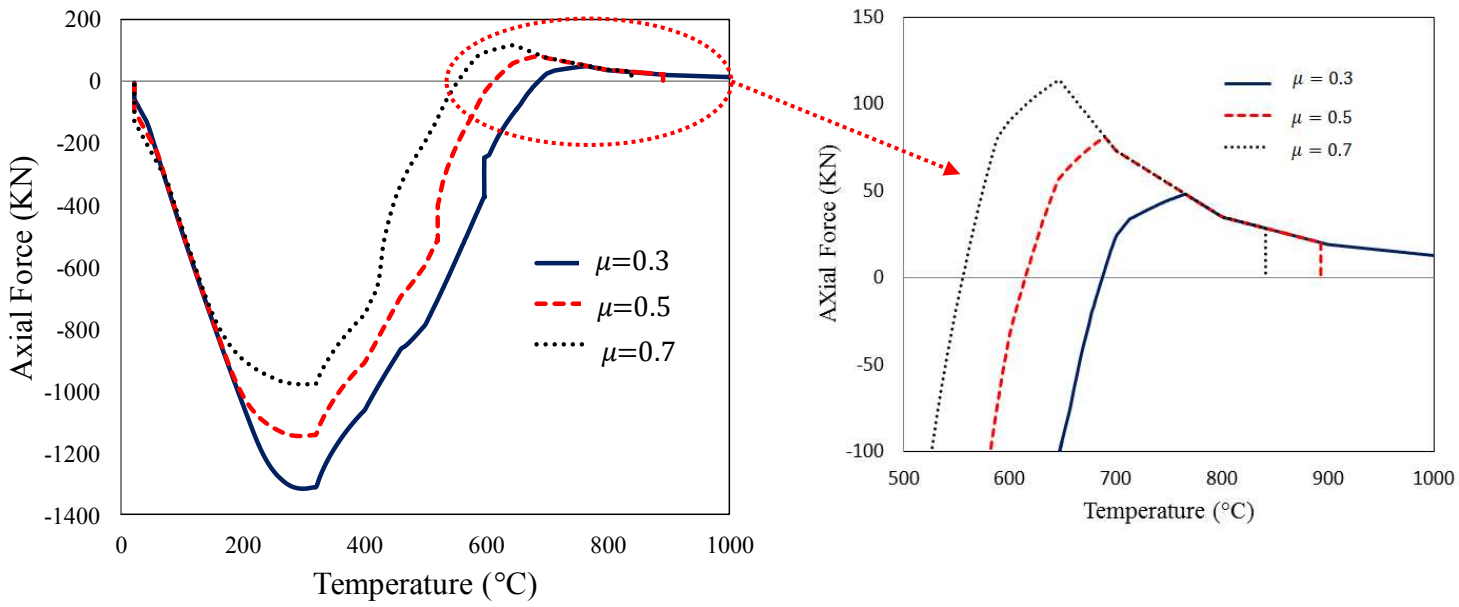

Figure 8 Normal forces in connections to beams with different load ratios.

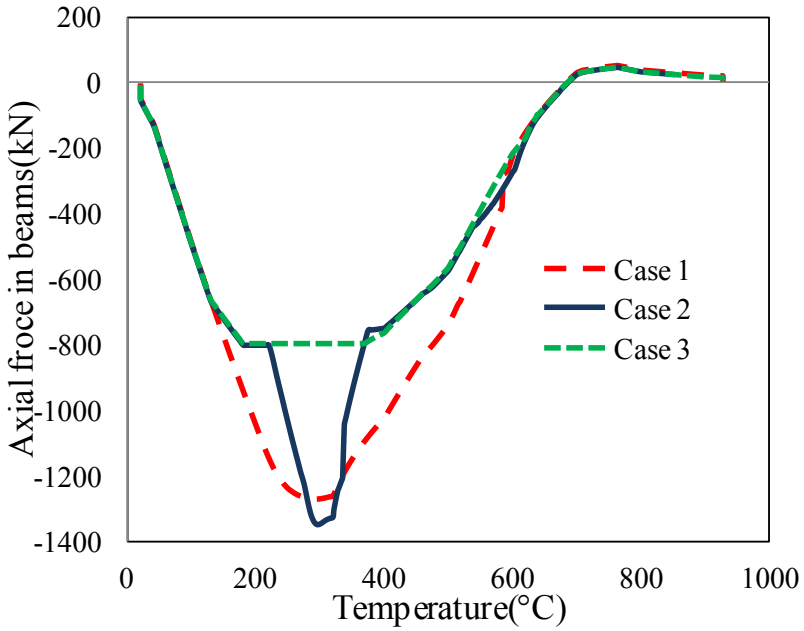

Figure 9 Axial forces at mid-span of the beam for different cases

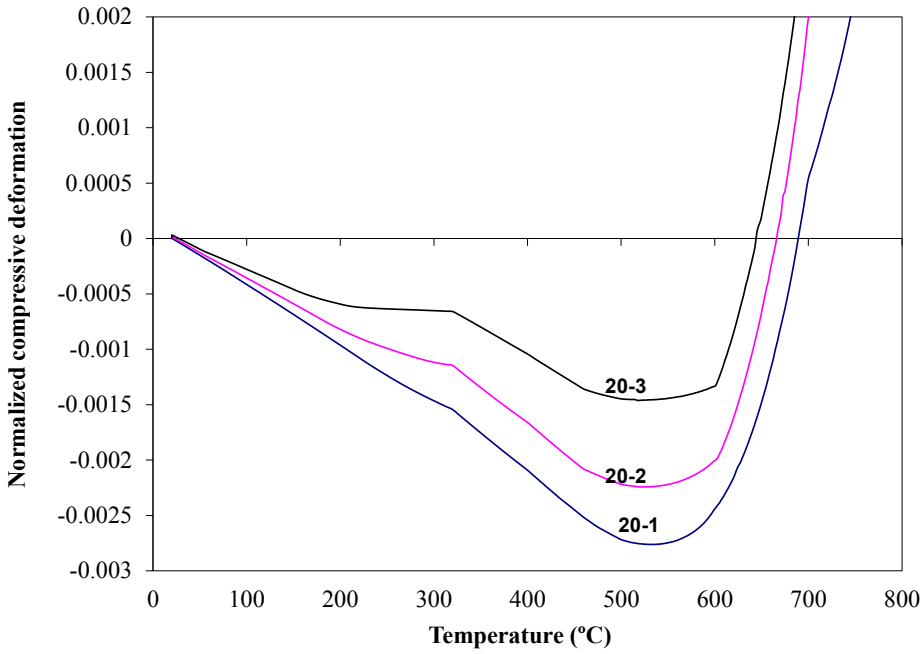
0.002
0.0015
0.001
0.0005
0
-0.0005
-0.001
-0.0015
-0.002
-0.0025
-0.003
Normalized compressive deformation
0
100
200
300
400
500
600
700
800
Temperature (ºC)
20-3
20-2
20-1

(a)

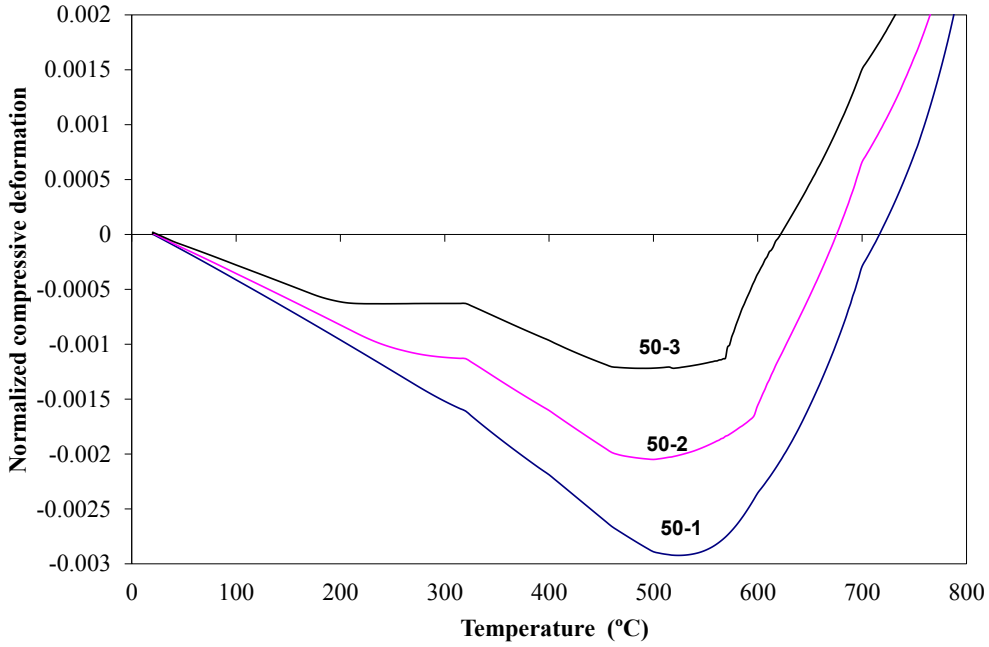
0.002
0.0015
0.001
0.0005
0
-0.0005
-0.001
-0.0015
-0.002
-0.0025
-0.003
Normalized compressive deformation
0
100
200
300
400
500
600
700
800
Temperature (ºC)
50-3
50-2
50-1

(b)

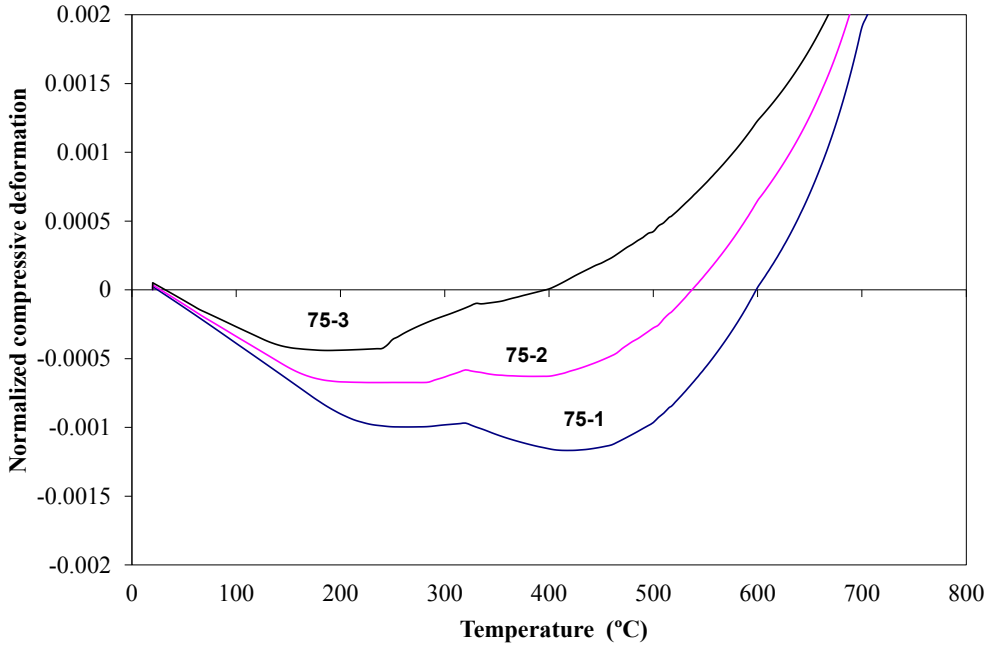

(c)

Figure 10 Normalized compressive deformation in the connections for different cases.

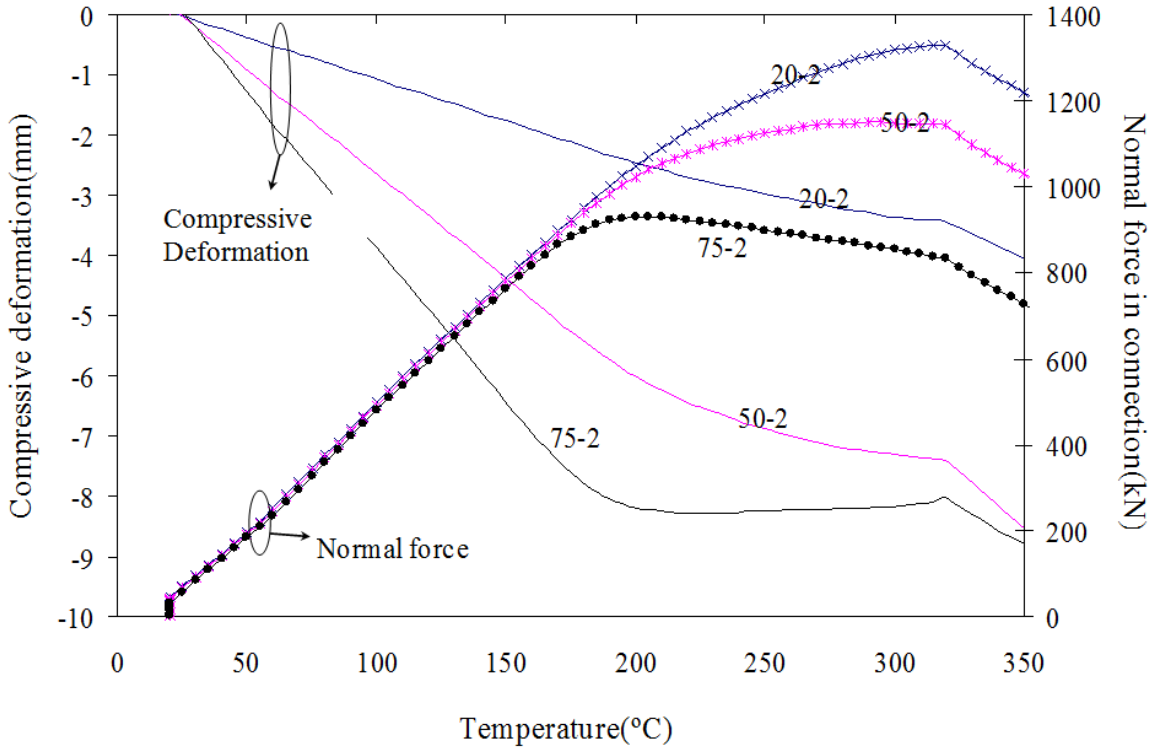

(a)

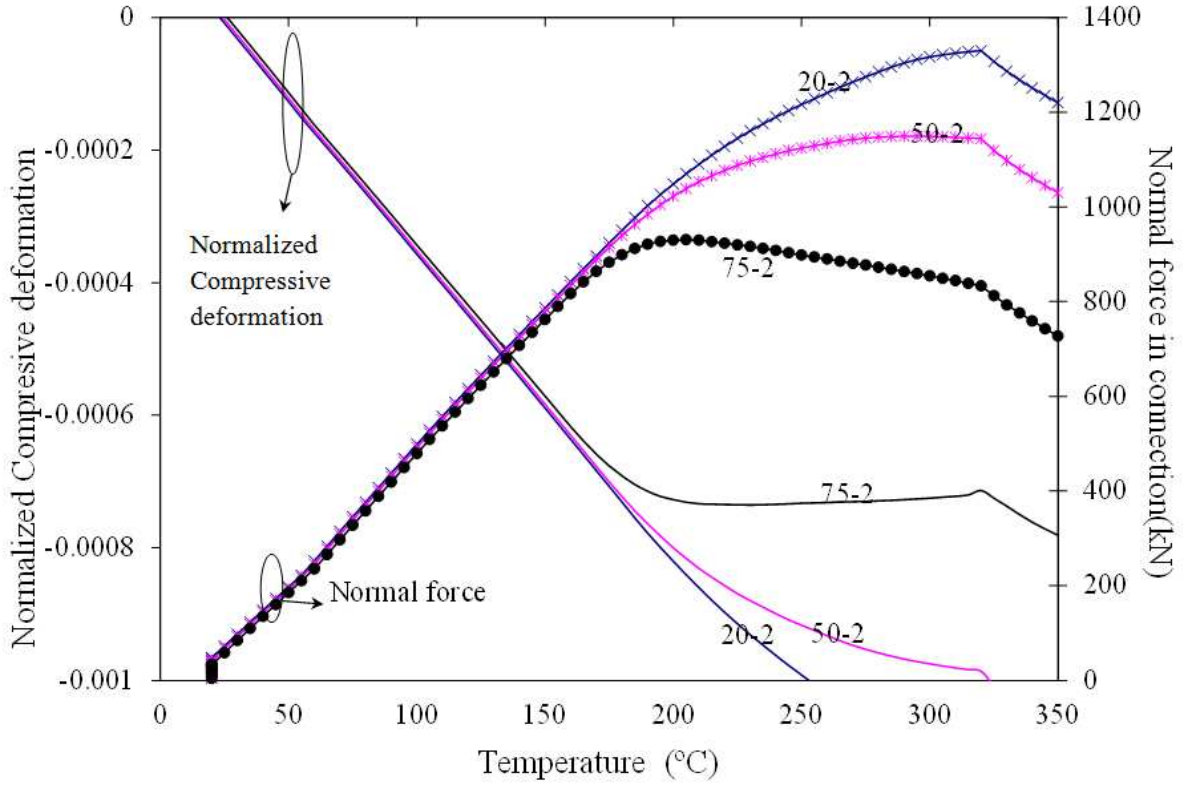

(b)

Figure 11 Compressive deformation (a) and normalized compressive deformation (b) in the connections for different cases

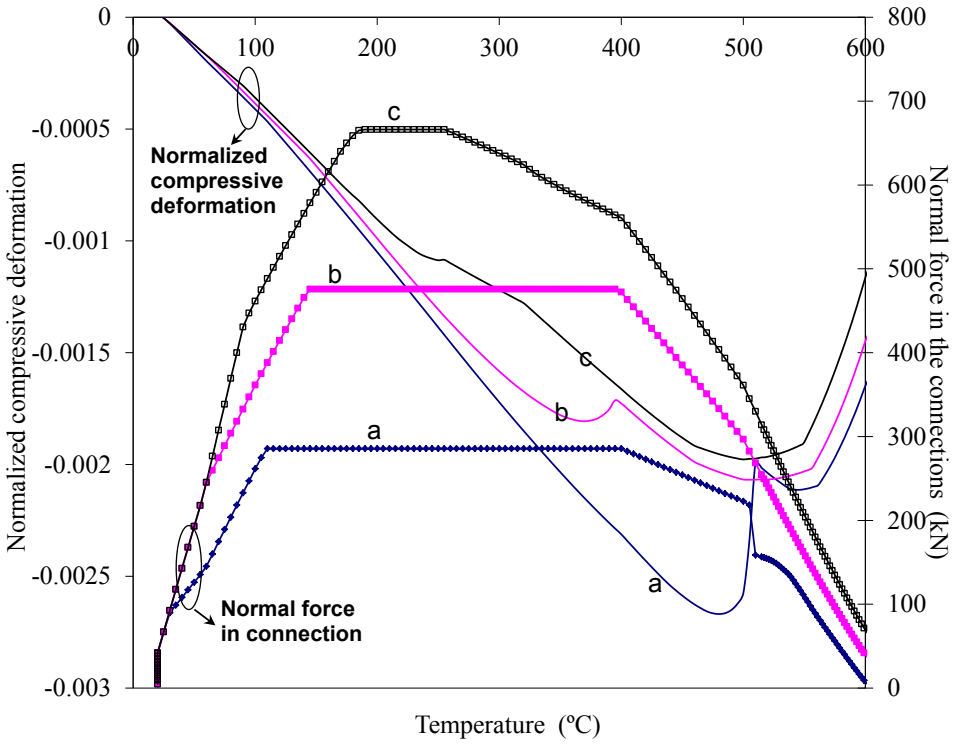

Figure 12 Compressive deformation in the connections for different cases